Physica Medica 59 (2019) 1–12

Contents lists available at ScienceDirect

Physica Medica

journal homepage: www.elsevier.com/locate/ejmp

Original paper

Characterizing a Geant4 Monte Carlo model of a multileaf collimator for a TrueBeam™ linear accelerator

Praneeth Kandlakunta, Shadab Momin, Austin Sloop, Tiezhi Zhang, Rao Khan*

Department of Radiation Oncology, Washington University in St. Louis School of Medicine, St Louis, MO, USA

ARTICLE INFO

Keywords:
Monte Carlo modeling
Linear accelerator
Multileaf collimator
Geant4 toolkit
Phase space
Dynamic simulation

ABSTRACT

Purpose: The purpose of this work was to develop and validate a multileaf collimator (MLC) model for a TrueBeam™ linac using Geant4 Monte Carlo (MC) simulation kit.

Methods: A Geant4 application was developed to accurately represent TrueBeam™ linac. Pre-computed phase-space file in a plane just above the jaws was used for radiation transport. A Varian 120 leaf Millennium™ MLC was modeled using geometry and material specifications provided by the manufacturer using Geant4 constructs. Leaf characteristics e.g. tongue-groove design, variable thickness, interleaf gap were simulated. The linac model was validated by comparing simulated dose profiles and depth-doses with experimental data using an ionization chamber in water. Dosimetric characteristics of the MLC such as inter- and intra-leaf leakage, penumbra effect, MLC leaf positioning, and dynamic characteristics were also investigated.

Results: For the depth dose curves, 99% of the calculated data points agree within 1% of the experimental values for the $4 \times 4\,cm^2$ and $10 \times 10\,cm^2$ and within 2% of the experimental values for 20×20, 30×30 and $40 \times 40\,cm^2$ jaw defined fields. The cross-plane dose profiles show agreement < 2% for depths up to 10 cm and to within 4% beyond 10 cm. MLC dosimetric characterization with MC agree well with film measurements. The rounded leaf penumbra remained constant throughout the range of leaf motion.

Conclusions: The TrueBeam™ linac equipped with 120-leaf MLC was successfully modeled using Geant4. The accuracy of the model was verified by comparing the simulations with experiments. The model may be utilized for independent dose verification and QA of IMRT.

1. Introduction

Monte Carlo (MC) techniques are known to provide the most accurate method for dose calculation in radiation therapy. Geant4 is a Monte Carlo toolkit for simulation of passage and interaction of particles with matter [1]. Geant4 is finding its use in medical physics research such as radiation therapy [2–7] owing to its extensive user-friendly features compared to other Monte Carlo codes. These include, for example, flexible geometry handling, extensively validated physics models [8–10], support for all types of particles, and ability to model sources and geometries in motion such as in IMRT, dynamic MLCs, brachytherapy sources and motion of patient organs during respiration [3].

Combinatorial and parameterized geometry techniques in Geant4 can be used for fast and effective definition of simple and regular geometrical shapes. Geant4 also has the ability to import CAD drawings in the form of tessellated solids into the MC model [11]. The ability to transfer the geometry from a CAD software to MC simulation environment is invaluable in case of a linac head model wherein the geometrical complexity of the components can be preserved to minimize geometry related errors and enable precise dose evaluation. Table 1 provides a brief summary of comparison of commonly used MC simulation codes in medical physics.

Due to the extremely favorable aspects of Geant4 for medical physics calculations, it has been used in some studies to validate the linac models [5,12,13].

Intensity modulated radiation therapy (IMRT) is a widely used advanced radiation therapy technique that precisely delivers radiation dose to the tumor while relatively sparing the surrounding normal tissues. Complex dose distributions in IMRT treatment are delivered using a multileaf collimator (MLC). The MLC undergoes complex motions during irradiation resulting in patterns of leaf movements depending on the complexity of objectives and the patient anatomy. Therefore, MC simulations may be used to independently verify dose calculations of the radiation therapy treatment planning systems. Additionally, the leaves of an MLC consist of complex structures such as the drive screw hole, rounded leaf end, tongue-groove design, leaf tip, support rail etc.

* Corresponding author.
E-mail address: khanrf@wustl.edu (R. Khan).

https://doi.org/10.1016/j.ejmp.2019.02.008
Received 17 October 2018; Received in revised form 11 February 2019; Accepted 12 February 2019
Available online 22 February 2019

Table 1
Summary of most commonly used MC codes in medical physics applications.

Feature	Geant4	MCNP	EGSnrc	PENELOPE
Access	Open Source (Free)	Licensed	Licensed-Freely distributed software	Licensed
CAD Import	Yes	Yes	No Direct CAD import	Import through triangle meshes
Software for CAD Import	InStep, SALOME, STViewer, FASTRAD, ESABASE2, CADMesh	MCAM, SuperMC, McCad, DAGMC	Component modules are developed separately, e.g. to model individual components in a Linac	PenMESH

The MLC leaves are generally characterized by certain dosimetric characteristics such as intra/inter leaf leakage, beam penumbra and tongue-groove effect. Detailed and accurate model of MLC is thus essential for radiation therapy planning owing to the MLC dosimetric characteristics that can result in significant contribution to the absorbed dose in normal and sensitive organs. On the other hand, the treatment planning systems are incapable of incorporating all details of an MLC. Thus, comprehensive modeling of the linac head including the MLC geometry is essential for accurate evaluation of IMRT dose distribution using MC simulations. For this purpose, an MLC model using MC simulations has been exclusively implemented for a TrueBeam™ linac in this work. There have been previous studies of MLC modeling using EGS4/BEAMnrc Monte Carlo code in literature, but to our knowledge, comprehensive MLC models involving dynamic motion using Geant4 have not been implemented. Heath et al developed a component model for dynamic MLC to be used with BEAMnrc simulations [14]. Jang et al developed and commissioned an in-house MLC model for IMRT using BEAMnrc code [15]. Recently, Onizuka et al (2018) used EGSnrc/BEAMnrc to verify VMAT plans for an Elekta linear accelerator equipped with 160-leaf MLC for dose validations [16]. A Monte Carlo dose calculation algorithm was developed for an MLC in robotic radiosurgery treatment planning whose accuracy was verified by comparing against film measurements in another recent study [17]. One study dealing with Geant4 and simplified version of Varian MLC on a Clinac™ has been reported [18]. In this study, we have developed a comprehensive MLC model for evaluation of IMRT dose on Varian TrueBeam™ linac. This required two separate modeling steps – evaluating the beam model when MLCs are parked and subsequently characterizing the MLCs to study their dosimetric impact.

2. Materials and methods

2.1. Monte Carlo model

A model of the TrueBeam™ linear accelerator was built using Geant4 v10.03 for a 6 MV clinical photon beam. Due to uncertainty in modeling linac head geometry upstream of the secondary collimators, we chose to use vendor provided phase space data located in a plane just above the secondary jaws. Geometry downstream of the phase space plane is modeled based on drawings and specifications provided in the Truebeam™ MC data package (Varian Medical systems, Palo Alto, CA). The accelerator model thus included the plane phase space source, the X and Y collimator jaws, the base plate supporting the jaws and the Millennium 120-leaf MLC (see Fig. 1).

The MLC was positioned at ~48 cm below the target and has been modeled in details by considering an interleaf air gap (0.0046 cm) and the tongue-groove design to preserve the geometrical accuracy (Fig. 2). This involved explicit modeling in the form of half-leaf isocenter, half-leaf target, full-leaf and outboard leaves. This was made possible by first creating simple solids with G4ExtrusionSolid and G4Tubs classes and then combining them with a Boolean operation using G4SubtractionSolid class. The MLC features included in the model were leaf tip, tongue, groove, screw hole and rails. The modeling of upper and lower jaws and the MLC with adjustable settings was facilitated by use of macros in Geant4 application. A number of user interface commands were written to configure different geometrical aspects of the model without requiring recompilation between runs.

For transport calculations we employed Geant4 standard electromagnetic_opt4 physics package. The package is designed to provide high accuracy simulation for electromagnetic models with multiple scattering and error-free stepping near the geometrical boundaries for all secondary particles. The range cut value was set at 0.1 cm. Particle phase space data above the jaws was available in the form of several phase space file pairs in IAEA format. Each pair consisted of a header file containing the number of particles and a binary phase space data file. Multiple phase space files were concatenated using an open source python script to yield a phase space with a size of 3.9 GB and consisting approximately 2×10^8 electrons and photons in total. The phase space files were read into the Geant4 model and primaries were generated using G4IAEAphspreader class. Particle recycling was used to simulate 1×10^9 primary events in the model. Simple geometry biasing was applied in the form of killer planes above the target and below the phantom, and killer surfaces around the accelerator to eliminate particles that are unlikely to contribute to the dose in the readout geometry of the phantom. The Geant4 model was built with the multithreading capability in Geant4 v10.03 to enable fast computations on multi-threaded CPUs.

2.2. Millennium 120-leaf multileaf collimator

The Millennium 120 leaf MLC consisted of two banks A and B containing 60 leaves each. Depending on the composition and leaf manufacturing of the tungsten alloy, the physical density can range from 17.15 to 17.85 g/cm^3. The leaves were categorized into four types, half leaf-target, half leaf-isocenter, full leaf and outboard leaf. Forty half leaves were positioned in the central part of the radiation field with each having a projected width of 5 mm at the isocenter. Eighteen full leaves and two outboard leaves were positioned on the outer part of the field, each with 1 cm width at the isocenter. The isocenter half leaf (thicker end towards the isocenter) and the target half leaves (thicker end towards the target) were arranged in an alternating form and together they formed adjacent pair. The leaf sides were focused toward the target to account for beam divergence and to minimize geometric penumbra across the leaves. Similarly, the leaf tips were rounded to keep approximately constant penumbra size for all leaf positions. A small air-gap exists between nominally closed pairs of opposing leaves from either banks to avoid collision between leaves. This abutting leaf gap along with rounded leaf tips accounts for significant leakage between each closed (opposing) leaf pair. Adjacent leaves within a bank were also separated by an interleaf air-gap to allow the leaves to slide past freely. Each leaf has a tongue and groove design to reduce interleaf leakage. The maximum open field projections of this MLC at the isocenter yielded 40×40 cm^2 field. MLC leaves move only along the x-direction parallel to the x-jaws.

2.3. Geant4 simulation

Dose calculations were typically performed in a $60 \times 60 \times 40$ cm^3

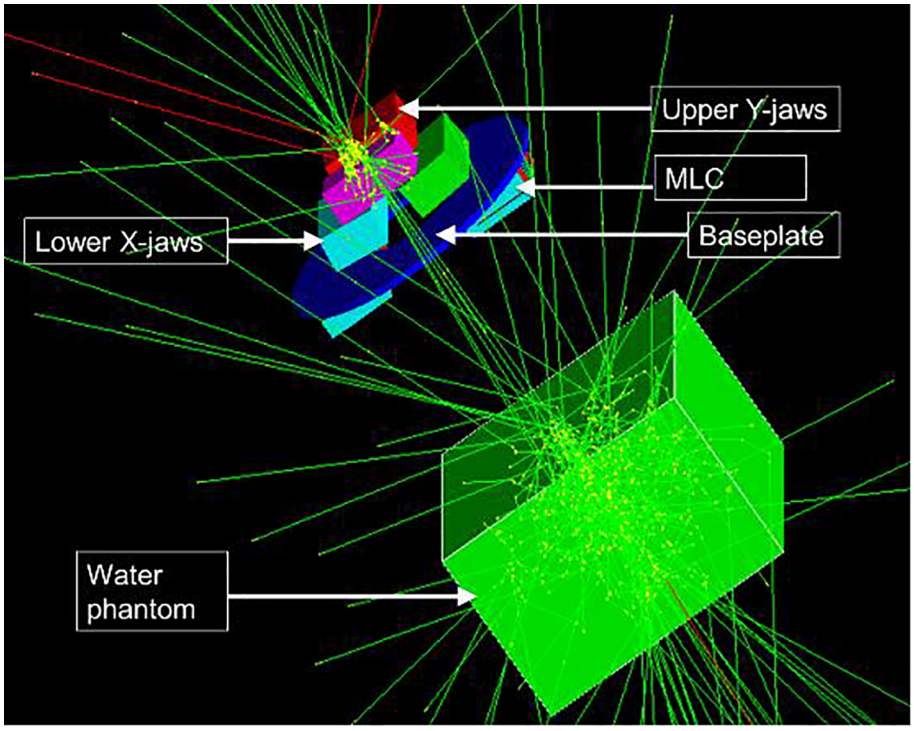

Fig. 1. Geant4 model of the TrueBeam™ Linac showing the accelerator components and a water phantom.

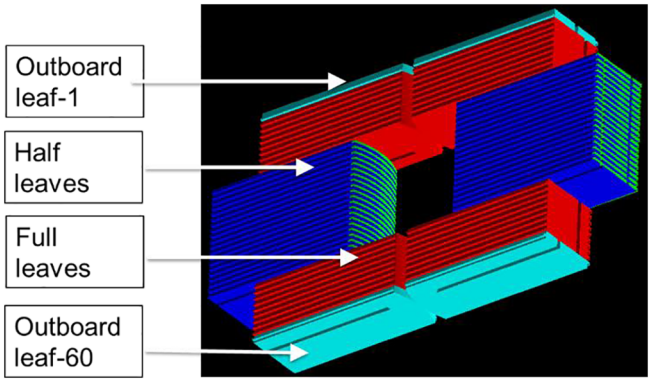

Fig. 2. Geant4 model of 120-leaf MLC.

water phantom in a sensitive detector readout geometry of variable size, for example with a voxel size of 0.3 cm for lateral dose profile and of 0.2 cm for percent depth dose calculations, respectively, in the scoring direction. Each Geant4 simulation was performed on a Geant4 virtual machine installed on a workstation with multicore, multi-threaded CPU (Intel Core i7 ePro) with an average computation time of ~12 h. There are two major aspects of this work – linac model validation, multileaf collimator specific simulations. The MLC model was evaluated by simulating various patterns to determine the impact of MLC transmission, inter- and intra-leaf leakage, dynamic leaf movements and leaf penumbra on dose calculation (*II.3.2* through *II.3.5*).

2.3.1. Validation of linac model

Percent depth dose and dose profiles at five different depths were calculated for the 6 MV beam for five square fields from $4 \times 4\,cm^2$ to $40 \times 40\,cm^2$ size. A source-to-surface distance (SSD) of 100 cm was used in the calculations. Data for depth-dose curves was normalized to the maximum value while the dose profile data was normalized to the dose value on the central axis.

2.3.2. MLC transmission and leakage

MC simulations were performed for a $10 \times 10\,cm^2$ blocked field with an abutting leaf air-gap of 0.1 cm and a leaf density of $17.7\,g/cm^3$ [14,19]. Longitudinal profiles were scored at 2 cm and 4 cm offsets from the central axis at 5 cm depth in a water phantom with a voxel size of 1 cm × 0.1 cm × 0.5 cm. Simulations were also performed for the same jaw setting and the MLC leaves closed to calculate the abutting leaf leakage profile. To evaluate the MLC penumbra, $10 \times 10\,cm^2$ MLC defined field with $15 \times 15\,cm^2$ jaws was modeled and dose was recorded in the water phantom at 5 cm depth.

2.3.3. Picket fence pattern

The picket fence pattern test provides a quick and efficient visual check of relative MLC leaf positions. In the present case, the picket fence pattern consisted of 1 mm wide strips at 2 cm intervals formed by closing the MLC leaf pairs while the jaws were set to $14 \times 40\,cm^2$ (X × Y) at the isocenter. The MLC test pattern implementing a picket fence dose distribution was modeled and calculated using the Geant4 simulation to validate the MLC model for dynamic MLC based IMRT. In this study, the dose distribution of the dynamic MLC fields was calculated by integration of segment dose distribution for each control point of the MLC pattern.

2.3.4. Impact of rounded leaf ends

In Varian MLC designs, the MLC leaf edges are rounded to keep an approximately constant penumbra for all leaf positions. This test evaluates the variation of leaf penumbra as a fixed MLC defined field is swept across the center of the radiation beam. Simulations were performed to evaluate the effect of change in leaf position on the penumbra size. MLC field size of $10 \times 10\,cm^2$ was used with jaw setting of $14 \times 14\,cm^2$. Five different asymmetric fields were created as the MLC leaves on one bank advanced by 2 cm while the leaves on the other bank retracted by 2 cm for each field, the isocenter remained fixed at the same position for all cases. The jaw positions were correspondingly shifted by 2 cm for each run. Simulations were scored in a water

phantom at 1.5 cm depth.

2.3.5. Dynamic MLC motion modeling

To replicate how IMRT uses the MLCs to modulate the dose to a region in the target, this simulation broke up the normally continuous movement of the MLC leaves into 20 steps of equal dose. A total of 2×10^9 primary events were simulated, with a computation time of ~36 h. Two dynamic patterns were investigated: a pyramid – where the MLC leaves open evenly from a starting closed position at the center to 11×11 cm^2 field; and a field where the leaves start behind the jaws on one side, create a 5 cm gap, and swept across the field such that both banks end on the opposite side of the jaw. For both patterns the jaws were set to 10×10 cm^2. Simulations were recorded in $0.5 \times 0.5 \times 1$ cm^3 voxels at 1.5 cm deep in a water phantom at SSD of 100 cm.

2.4. Ion chamber and film measurements

The linac and the MLC models are validated by comparing calculated doses against the experimental measurements. Measurements of percent depth dose and dose profiles were performed using a CC13 (IBA, Reston, VA) ionization chamber in a water phantom at 100 cm SSD. The active volume of the ion chamber is about 0.13 cm^3. The measurement of depth doses and profiles with ionization chamber results in experimental uncertainty of ± 1%.

Measurements for MLC were performed using radiochromic EBT3 (International Specialty Products, Wayne, NJ) films positioned in a solid water phantom at depths matching those in the simulations. The films were processed on an EPSON 10,000 XL(Long Beach, CA, USA) flat-bed scanner and analyzed. The total experimental uncertainty associated with the film irradiation, scanning procedure and dosimetry is estimated to be around ± 3% [23].

Simulation parameters for the MLC model namely, abutting leaf gap and MLC material density are verified by comparing calculated and measured MLC leakage profiles. The interleaf leakage and abutting leaf leakage were measured with the film (10″ × 8″) at 5 cm depth in solid water. The abutting leaf leakage was measured with the jaws opened to 10×10 cm^2, the MLC leaves closed at the center and a film exposed to 400 MU. The interleaf leakage was measured with the jaws at 10×10 cm^2, the MLC leaves closed beyond the jaws (i.e. blocking the field) and a film exposed to 4800 MU. A reference measurement was performed with the same jaw setting and the MLC leaves fully retracted exposing a film to 100 MU. The irradiated films were subsequently scanned using the scanner for the analysis. The abutting leaf leakage profile was extracted from the scanned film under the center of a leaf pair. The interleaf leakage profile was extracted at 2 cm and 4 cm offset from the central axis in the direction of leaf travel. A large (13″ × 17″) film was irradiated at 100 cm SSD with 1200 MU to produce a picket fence pattern. For the rounded leaf end investigations, films were placed at the isocenter at 1.5 cm in a solid water phantom with an SSD of 98.5 cm and irradiated with 200 MU. For the dynamic MLC motion 400 MU were delivered under the aforementioned setup.

3. Results

Since Geant4 simulations involved a comprehensive model of linac head including the multileaf collimators, it was imperative to evaluate the beam model separately in order to avoid complexity arising from the MLC in the beam. This was accomplished by studying the linac model while the MLC were parked behind the jaws.

3.1. Linac model

The water phantom depth dose results are shown in Fig. 3(a), and the dose profiles in the phantom are shown in Figs. 4(a)–8(a) for depths ranging from 1.5 cm to 30 cm, respectively, for different square fields. Figs. 3(b) and 4(b)–8(b) show the ratio of Geant4 calculation to measurement data for depth dose distribution and for cross plane dose profiles, respectively. In order to ensure a statistical accuracy of within 2%, a minimum of 2×10^8 histories were required for 4×4 cm^2, while larger field size 40×40 cm^2 required up to 1×10^9 histories to achieve the same level of accuracy. For the depth dose curves, 99% of the calculated data points agree to within 1% of the experimental values for the 4×4 and 10×10 cm^2 fields and within 2% of the experimental values for 20×20, 30×30 and 40×40 cm^2 field sizes as illustrated in Fig. 3(b).

Gamma analysis was also performed to compare depth dose data with those of measurements. A gamma criteria of 2% dose difference and 1 mm distance to agreement was used for evaluation. For 4×4 cm^2 field, 98% of the points passed the gamma test, while 97.3% of points passed the test for 10×10 to 40×40 cm^2 fields. For the lateral dose profiles, the gamma score with the same criteria indicated 92% of points pass the test for 4×4 cm^2 field at 1.5 cm depth. The low gamma passing percentage is because points located in umbra and penumbra region have larger statistical uncertainties than those within the field. In general, for lateral dose profiles, the agreement is better than 2% (i.e. dose difference is ≤2%) within the field size for about 98% of calculated data for depths up to 10 cm. At depths equal to or greater than 20 cm, maximum dose difference is within 4% for all the field sizes. This is because at greater depths in water phantom, the attenuation of photons increases resulting in lower numbers of particles to score causing an increase in statistical uncertainties. The overall uncertainty in results is also influenced by other factors including model approximations, input phase space data, material composition, choice of the physics list and range cutoff in Geant4 etc.

3.2. MLC transmission and leakage

The geometry and materials comprising the MLC in our model were represented as per manufacturer's specifications. The simulation parameters such as abutting leaf gap were adjusted in order to minimize the discrepancy between the measurements and calculations. To investigate the effect of the abutting leaf gap a closed MLC field and for determining interleaf leakage, the MLC blocking an open field were simulated. The closed and blocked fields were both compared with film measurements in a solid water phantom at 5 cm depth and 95 cm SSD.

Abutting leaf leakage profile was scanned right under a leaf pair. Fig. 9(a) shows the EBT3 film irradiated for this measurement. Fig. 9(b) shows a comparison of the measured and calculated leakage profile underneath an abutting leaf pair. Simulation results are in good agreement with the film measurement. However, the film appears to overestimate the dose in the region below the leaf pair away from the leaf opening. The deviations between the two results in this region may be due to the film uncertainty, which, in general, is high at low dose levels [22]. A significant fraction 22% of the open field dose passes through abutting leaf air-gap or is transmitted through rounded leaf edges. The leakage between closed opposing banks of leaves arise from the fact the MLC banks are not fully closed in order to avoid any collisions. Typically this gap is of the order of 0.4–0.6 mm for Varian MLCs. In addition to the gap, the vendor implements an MLC leaf offset table at the MLC controller level, where the leaves are offset by the tabulated amount depending on their position. This attempts to maintain a constant relationship between field size FWHM and MLC positions.

Fig. 9(c) shows the EBT3 film irradiated for observing the MLC intra- and inter-leaf leakage. Fig. 9(d) and (e) show comparisons for the MLC intra- and inter-leaf leakage profiles in the longitudinal direction of the MLC blocked field (the jaws were set to 10×10 cm^2). The data acquired were normalized for comparison with the simulated profiles. Both figures indicate, peaks and valleys occurring approximately at the

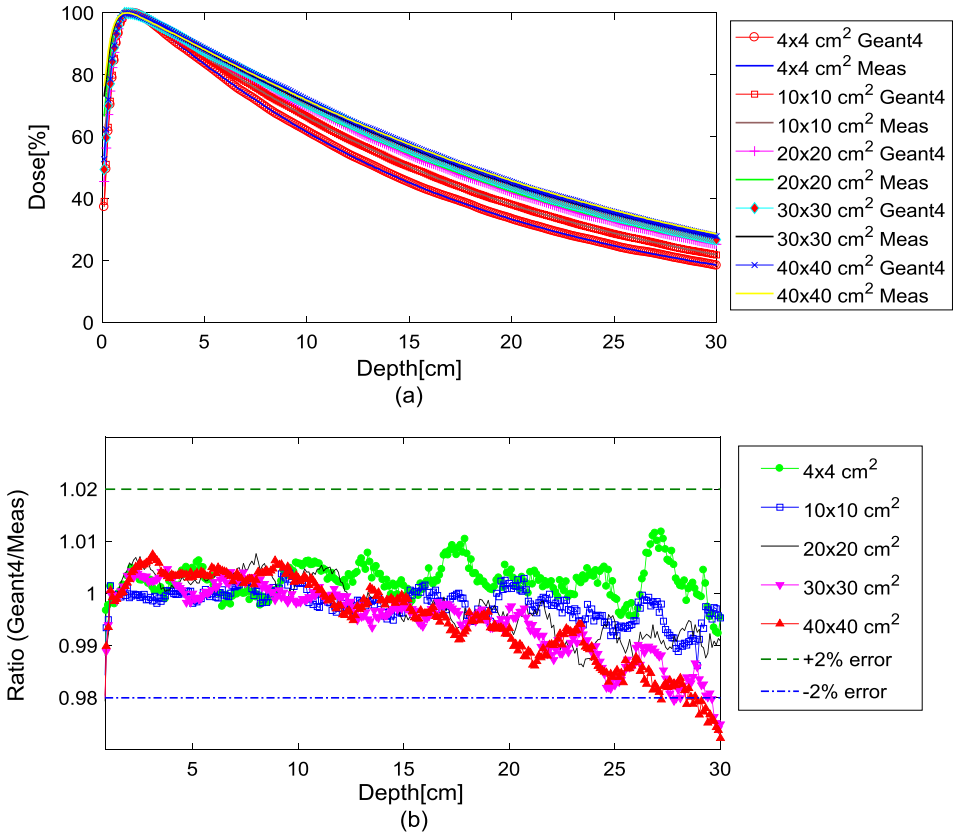

Fig. 3. (a) Measurement (lines) and Geant4 (line + symbol) calculated depth dose distributions for 6MV photon beam. (b) Ratio of Geant4 calculated data to ion chamber measurements for the percentage depth dose. Dotted lines are drawn at ± 2% as a visual guidance.

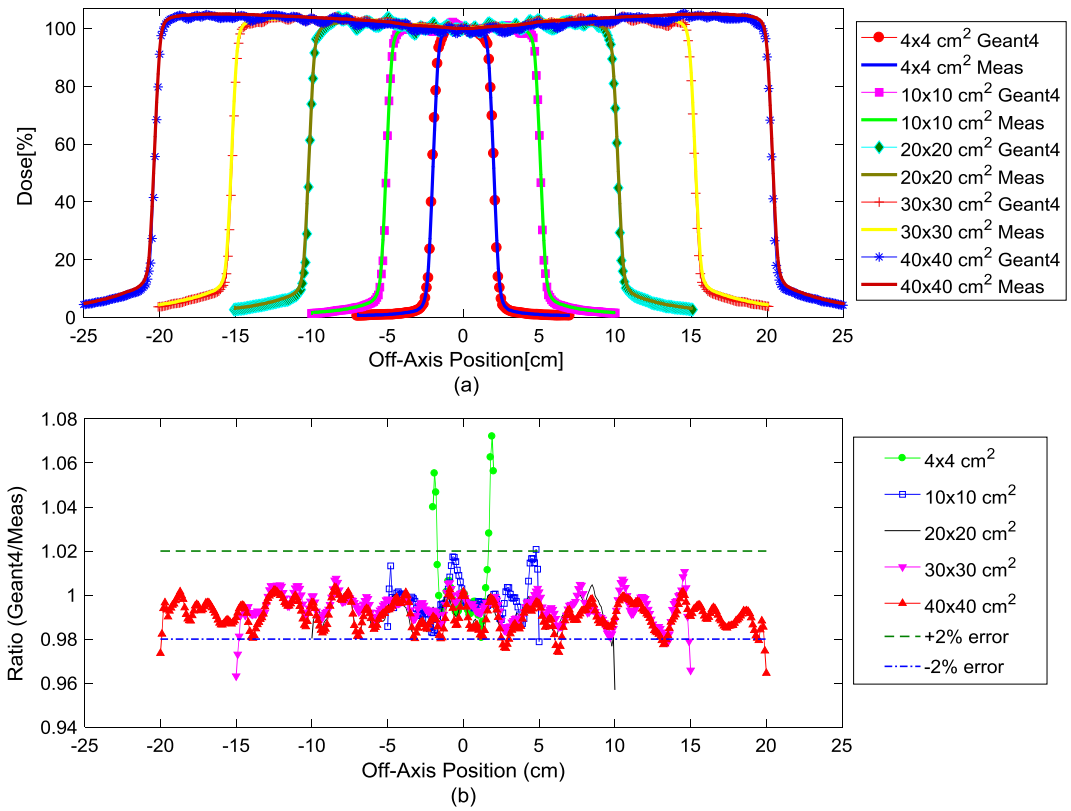

Fig. 4. (a) Measurement (lines) and Geant4 (line + symbol) calculated dose profiles at 1.5 cm depth in water phantom for different field sizes. (b) Ratio of Geant4 calculated data to measurement data for dose profiles at 1.5 cm depth in water phantom. Dotted lines are drawn at ± 2% as a visual guidance.

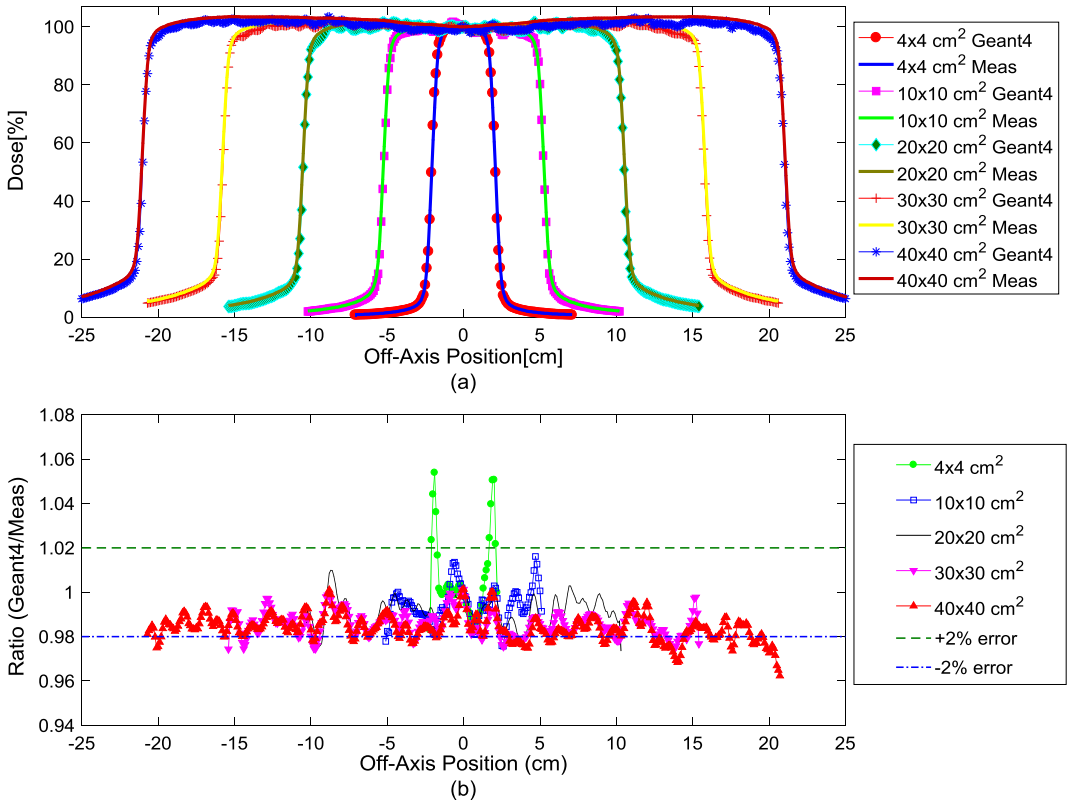

Fig. 5. (a) Measurement (lines) and Geant4 (line + symbol) calculated dose profiles at 5 cm depth in water phantom. (b) Ratio of Geant4 calculated data to measurement data for dose profiles at 5 cm depth in water phantom. Dotted lines are drawn at ± 2% as a visual guidance.

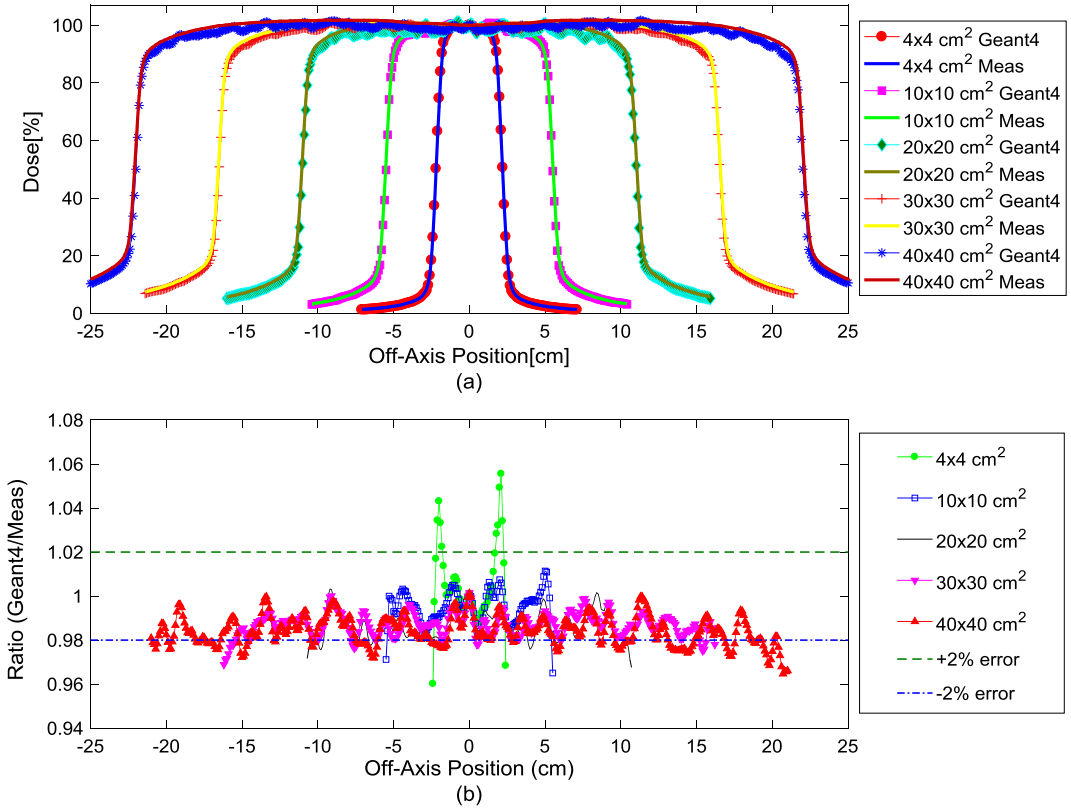

Fig. 6. (a) Measurement (lines) and Geant4 (line + symbol) calculated dose profiles at 10 cm depth in water phantom. (b) Ratio of Geant4 calculated data to measurement data for dose profiles at 10 cm depth in water phantom. Dotted lines are drawn at ± 2% as a visual guidance.

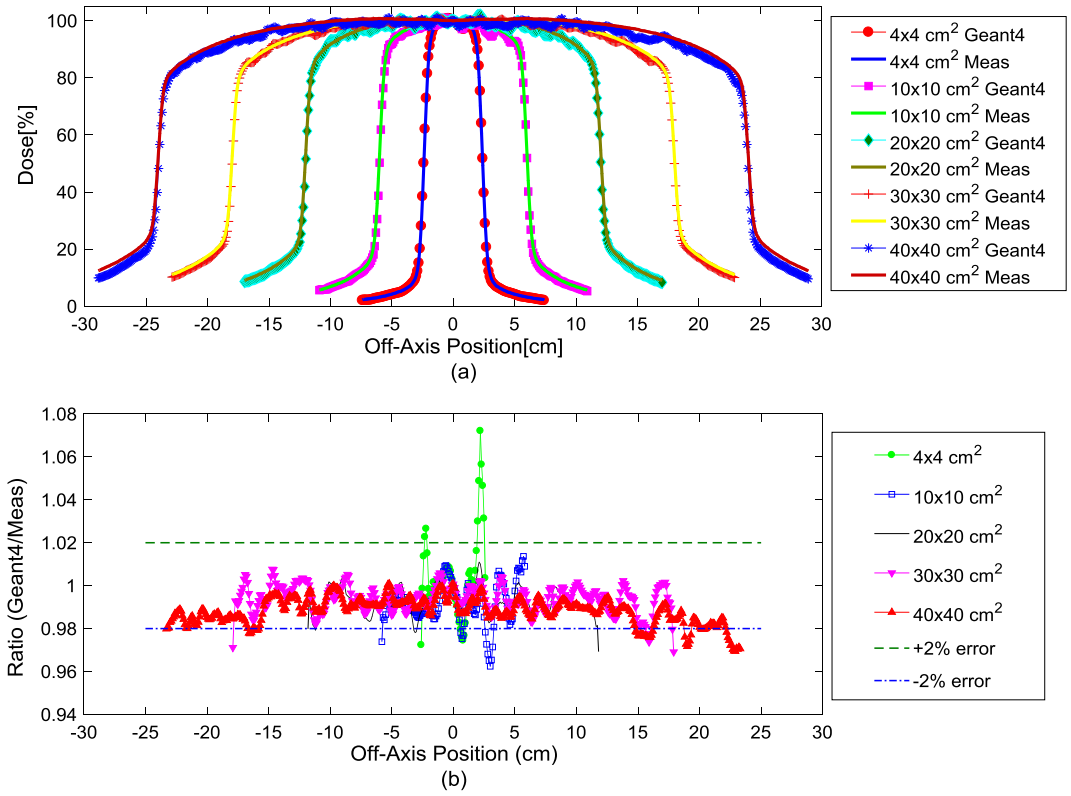

Fig. 7. (a) Measurement (lines) and Geant4 (line + symbol) calculated dose profiles at 20 cm depth in water phantom. (b) Ratio of Geant4 calculated data to measurement data for dose profiles at 20 cm depth in water phantom. Dotted lines are drawn at ± 2% as a visual guidance.

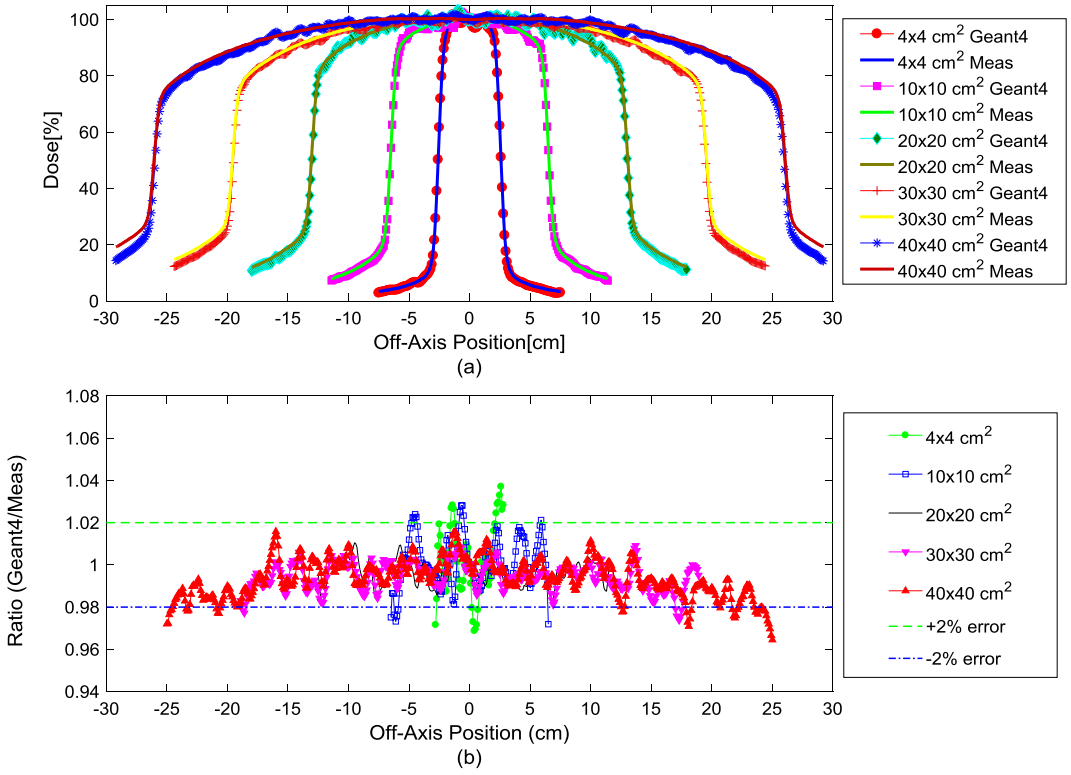

Fig. 8. (a) Measurement (lines) and Geant4 (line + symbol) calculated dose profiles at 30 cm depth in water phantom. (b) Ratio of Geant4 calculated data to measurement data for dose profiles at 30 cm depth in water phantom. Dotted lines are drawn at ± 2% as a visual guidance.

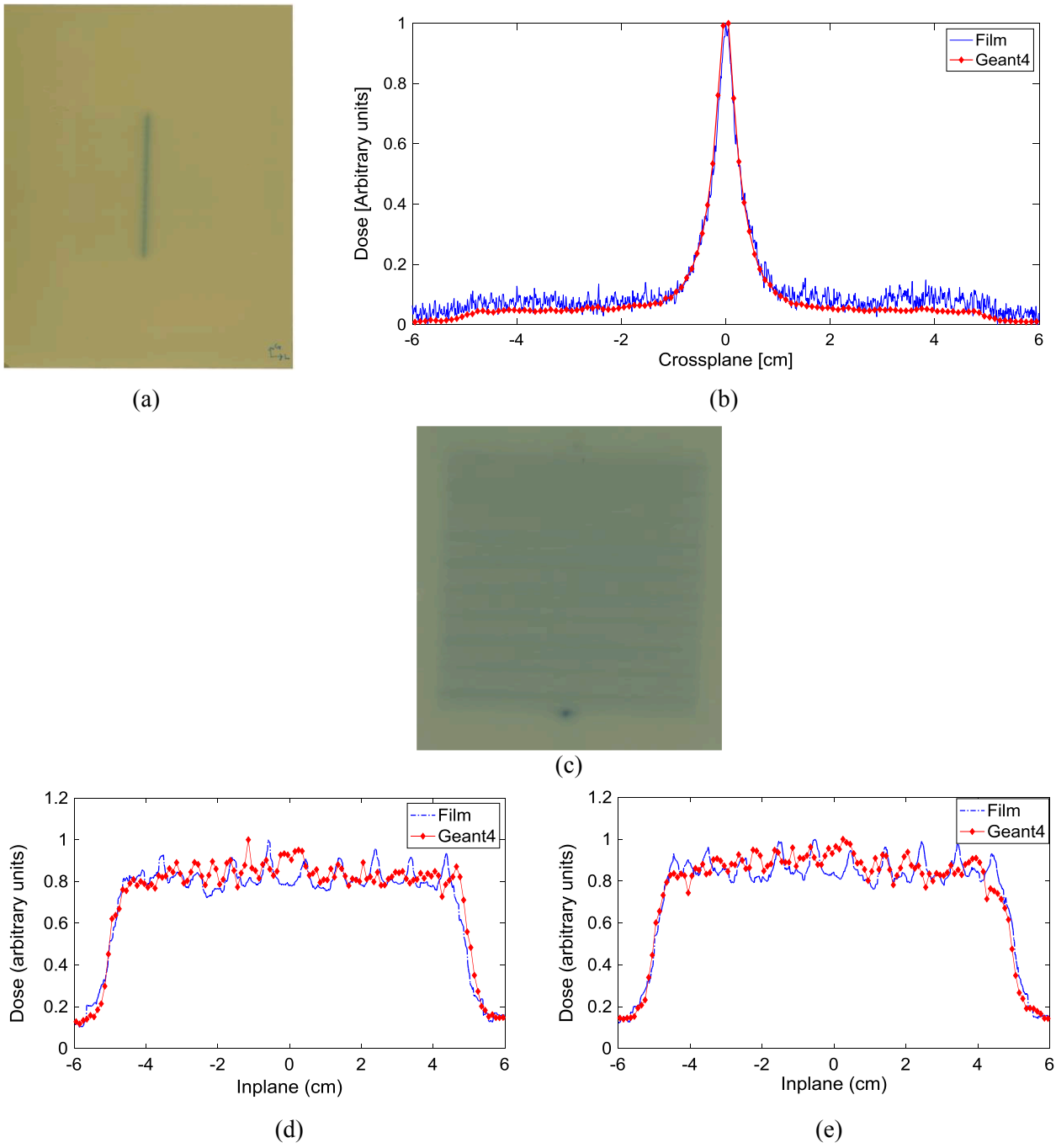

Fig. 9. (a) Film measurement with closed MLC leaves. (b) Abutting leaf leakage profile under a leaf pair. (c) Film measurement with MLC leaves blocking an open field. Interleaf leakage profiles at (d) x = 2 cm and (e) x = 4 cm offset from the central axis.

same position for both profiles, which corresponds to the inter-leaf and intra-leaf leakage, respectively. The Geant4 calculations are generally in good agreement with the film within the field, while slight discrepancy may be attributed to the uncertainties in film dosimetry. For 6MV beam, the MLC transmissions results in 1.46% for simulation and 1.54% from measurement.

3.3. Picket fence pattern

Fig. 10(a) and (b) show the dose distributions calculated Geant4 simulation and measured by EBT3 films respectively for a picket-fence MLC pattern. Fig. 10(c) compares the cross plane dose profiles for simulation and measurements. It can be seen that measurement results and simulation are in very good agreement, while the noise in the measurement can be attributed to the film.

3.4. Impact of rounded leaf ends

Fig. 11 shows cross-plane dose profile in the MLC dose region for the evaluation of static leaf penumbra for a symmetric MLC defined field about the central axis. The Geant4 simulation result (red color) is in good agreement with the film measurement result (green color).

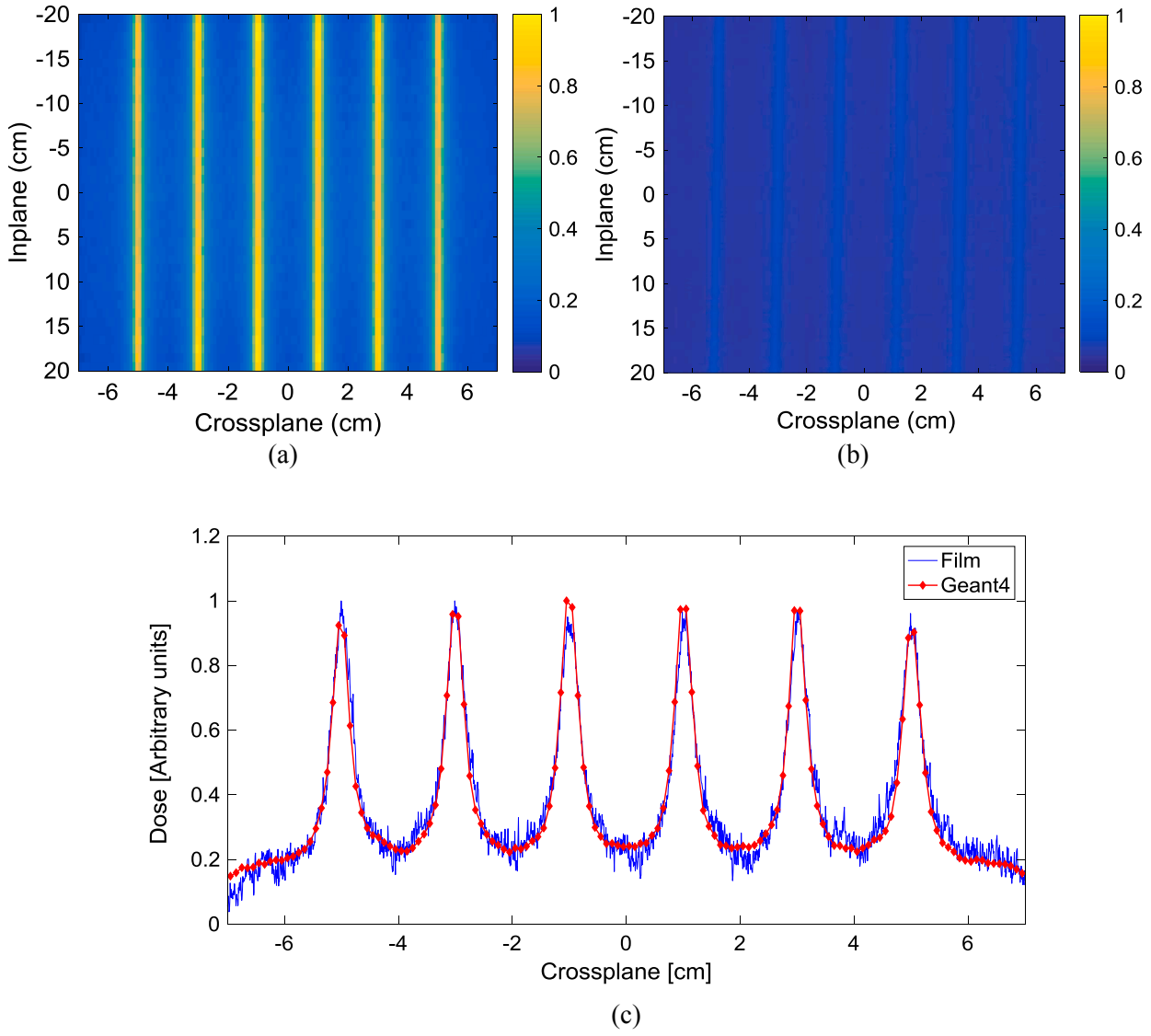

Fig. 10. Dose distribution of a Picket fence pattern calculated using (a) Geant4 simulation and measured with (b) EBT3 film. (c) Comparison of a cross plane profile of the picket fence pattern from Geant4 simulation and measurement.

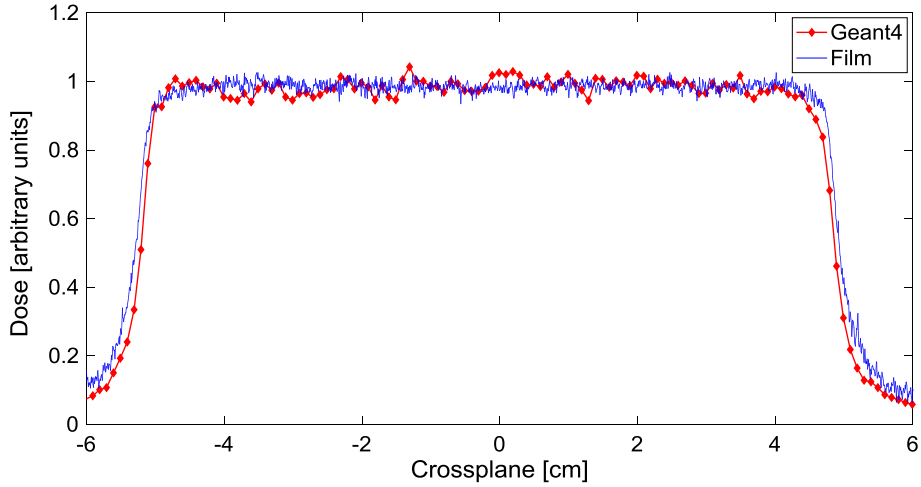

Fig. 11. Cross plane profile for the evaluation of MLC penumbra. (For interpretation of the references to color in this figure legend, the reader is referred to the web version of this article.)

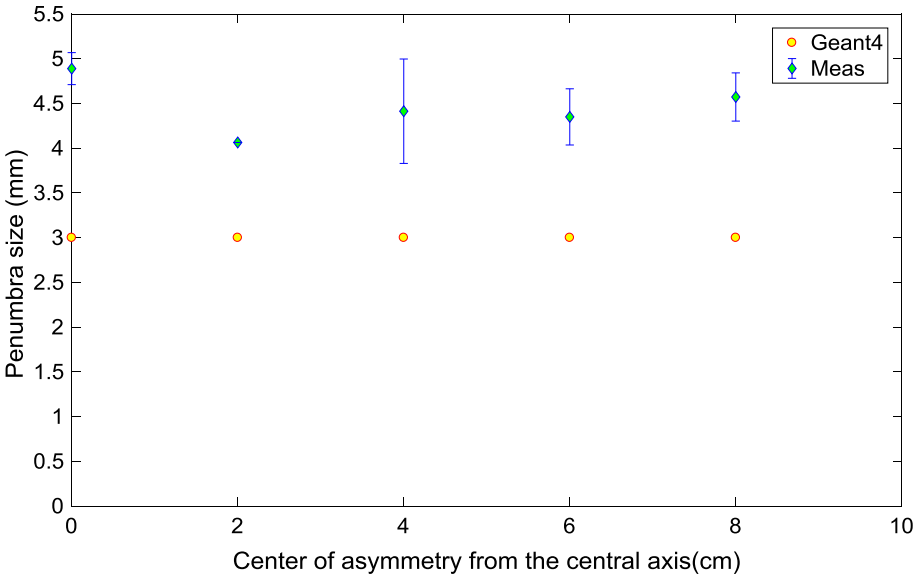

Fig. 12. Variation in penumbra width with the center of asymmetry.

In order to study the travelling leaf penumbra, a $10 \times 10\,cm^2$ MLC defined field was positioned at various locations from the field center. The 80–20% penumbra size for each MLC field obtained from simulations and measurement is shown in Fig. 12 as the center of the asymmetric field varies. The penumbra size from the film measurements varies between 4 and 5 mm, whereas the simulations indicate an almost constant penumbra of 3 mm. The difference may be attributed to approximations made in representing MLC round leaf edges and the radius of curvature in simulations, and uncertainty in the film measurement. Results in Fig. 12 also indicate that although the rounded leaf ends of Varian MLC are designed to follow beam divergence and maintain approximately constant penumbra size for all leaf positions, the penumbra width in reality is affected by the leaf positions.

3.5. Dynamic MLC motion modeling

The water phantom dose profiles for a pyramid MLC pattern are shown in Fig. 13(a). Fig. 13(b) shows the ratio of the Geant4 calculation to film measurements for the same cross plane profile. The profiles show an excellent agreement with the film measurements in general. However, for the regions close to the X jaws the disagreement increases up to 6%.

The cross plane dose profile for the sliding window motion of the MLC is shown in Fig. 14(a) along with relative discrepancies between simulations and measurements for the $10 \times 10\,cm^2$ field in Fig. 14(b). Most of the disagreement may be attributed to the stepping artifacts used as an approximation of continuous DMLC motion. The striations in both the film and simulations occurred at different × positions possibly due to slight differences in penumbra location of the leaves. However, the overall field penumbra for the film (0.35 ± 0.02) and simulations (0.38 ± 0.01) were in good agreement.

4. Discussion and conclusions

The MLC is a crucial and integral part of the linacs for delivery of IMRT dose distributions, demanding highly accurate dose modeling in order to fully realize their potential. The MLC model in MC system is an approximation of physical representation of MLCs mounted in the linac head. Several MLC models via MC simulation have been developed in the past. These works include modification in fluence intensity without simulation of transport through MLC geometry [24], simplified transport calculation [25] and more detailed modelling of MLC for BEAMnrc module [14]. Modeling the MLC via MC simulation can provide greater confidence in computed dose especially for small field. The small fields have now become very important especially in IMRT and VMAT era. In this study, we developed a 6MV MC model of linac equipped with 120-leaf MLC using Geant4 toolkit as independent dose verification and quality assurance tool for IMRT. The study was performed in two phases: development and validation of a TrueBeam™ radiation beam model while MLCs are parked; development of Millennium MLC model and its characterization. Ionization chamber measurements were used to validate the beam model for our simulations, whereas film measurements were performed to evaluate Geant4 simulations of MLC leakage, penumbra and dynamic MLC patterns.

For jaw defined fields, the Monte Carlo calculations were found to be in agreement with ionization chamber measurement to within 2% for PDD and < 4% for the dose profiles. These results indicated proper modelling of shape and materials of the target used in the simulation. The implementation of MLC model was validated by assessing abutting leaf leakage, interleaf leakage, penumbra and picket fence pattern, and dynamic motion patterns. Overall results of these tests in the second phase of this study indicated a reliable modelling of the MLC.

One major limitation of MC simulations is the computation time. Although pre-calculated phase space data were used as a particle source, recording dose in a voxelized phantom still takes an unreasonable amount of time. This work focused mostly upon incorporating the modeling details of the MLC. Accelerating the computation was not a major objective of this work, which could perhaps be achieved using various variance reduction techniques in addition to utilizing more powerful computational resources. In general, our results were in line with other linac models reported in the literature [21]. Compared to Borges et al [21], our work involved vendor provided phase space files and the Varian 120 leaf Millennium model of MLC, which is more commonly used for IMRT treatments. This model required four different formulations for various leaf types used. Our tongue and groove model was based on using Geant4 geometry constructs. Another source of uncertainty may be extensive reliance on vendor supplied information in the form of phase-space files, which may conceal the level of modeling details (upstream of jaws) used to generate it. In another recent work Perales et al [20] reported a comprehensive validation of Siemens Oncore Impression Plus linac with a 160 leaves MLC having a tilt-leaf design (thickness diverging leaves away from the radiation source) with Geant4. While Perales et al. [20] investigated the influence of modelling parameters on dose calculation,

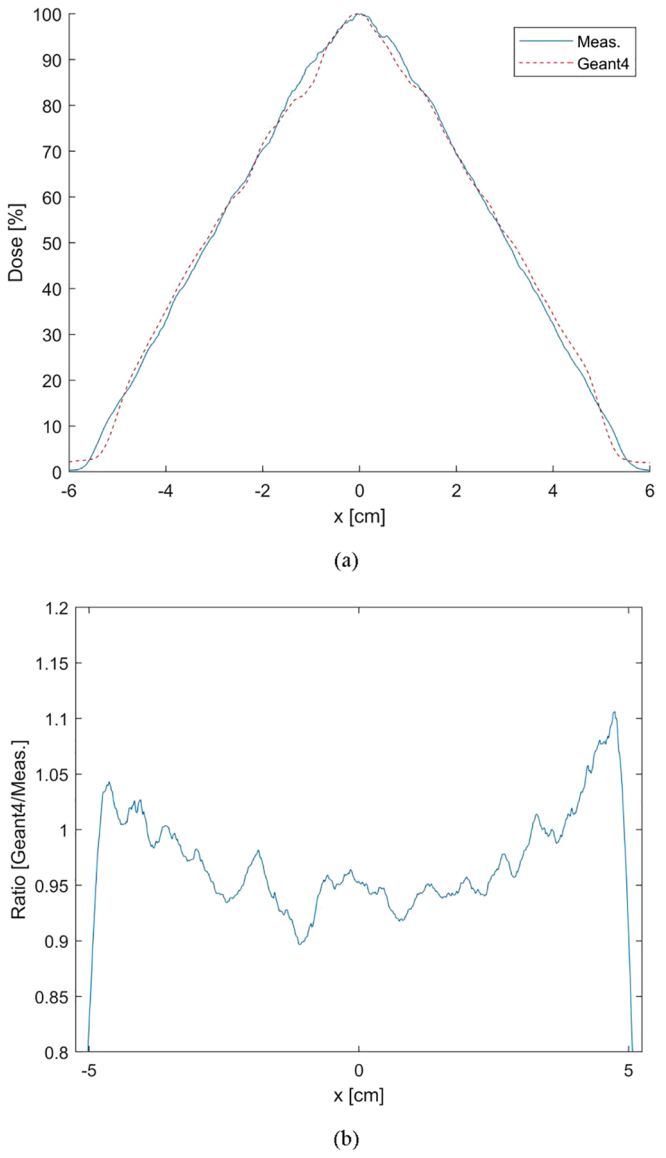

Fig. 13. (a) Measurement (lines) and Geant4 (dashed) calculated dose profiles at 1.5 cm depth in water phantom for pyramid DMLC simulation. (b) Ratio of Geant4 calculated data to measurement data for dose profiles at 1.5 cm depth in water phantom.

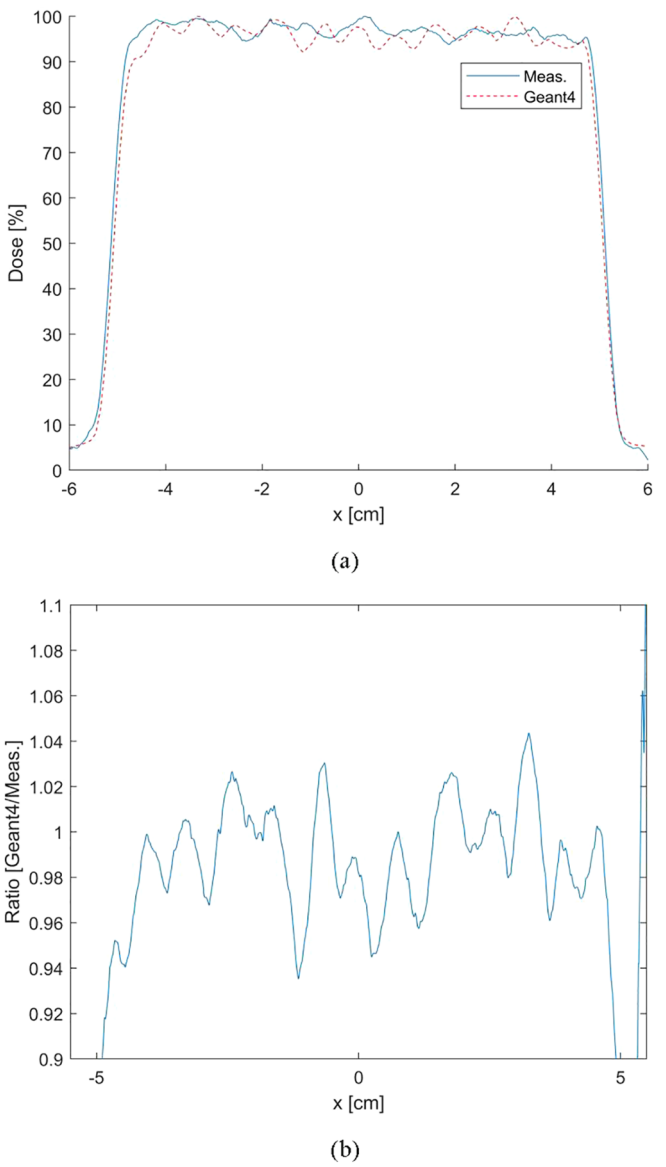

Fig. 14. (a) Measurement (lines) and Geant4 (dashed) calculated dose profiles at 1.5 cm depth in water phantom for sliding window DMLC. (b) Ratio of Geant4 calculated data to measurement data for dose profiles at 1.5 cm depth in water phantom for sliding window DMLC.

this study focused on implementing and verifying detailed MLC model in addition to developing and validating the beam model, with the aim of its potential use as a QA tool. One important issue that needs attention is the inter-leaf gap between adjacent leaves. The vendor supplied leaf drawings may only provide the machined dimensions of a leaf, however, the additional leaf coating is typically not made available readily. By ensuring the alignment of outer-leaves with the frame of the MLC housing and optimizing both the leaf thickness and air-gap between them iteratively, inter-leaf leakage and alignment can be matched. Though in this work, we resorted only to optimizing the air-gap. Though, the level of detail in the current model is accurate to within the dosimetric measurement uncertainties, using a CAD based import feature of the Geant4 one should be able to incorporate finer details such as small straight parts on MLC tip in addition to the rounded end.

In this study, the Varian 120 Millennium MLCs were modeled in detail on a Monte Carlo Geant4 system. The results of the validation of the MLC model proved its reliability in accurately calculating the dose distributions for both static and dynamic MLC movements. The results of current study, therefore, suggest its potential use to perform independent quality assurance simulations for patient dose calculations in IMRT and VMAT.

Appendix A. Supplementary data

Supplementary data to this article can be found online at https://doi.org/10.1016/j.ejmp.2019.02.008.

References

[1] Agostinelli S, Allison J, Ka Amako, Apostolakis J, Araujo H, Arce P, et al. GEANT4 – a simulation toolkit. Nucl Instrum Meth Phys Res A 2003;506:250–303.
[2] Foppiano F, Mascialino B, Pia M, Piergentili M. A Geant4-based simulation of an accelerator's head used for intensity modulated radiation therapy. Nuc Sci Symp Conf Rec 2004:2128–32.
[3] Paganetti H. Four-dimensional Monte Carlo simulation of time-dependent geometries. Phys Med Biol 2004;49:N75.
[4] Jiang H, Paganetti H. Adaptation of GEANT4 to Monte Carlo dose calculations based on CT data. Med Phys 2004;31:2811–8.
[5] Constantin M, Perl J, LoSasso T, Salop A, Whittum D, Narula A, et al. Modeling the TrueBeam linac using a CAD to Geant4 geometry implementation: dose and IAEA-

compliant phase space calculations. Med Phys 2011;38:4018–24.
[6] Spiga J, Siegbahn E, Bräuer-Krisch E, Randaccio P, Bravin A. The GEANT4 toolkit for microdosimetry calculations: application to microbeam radiation therapy (MRT). Med Phy 2007;34:4322–30.
[7] Archambault L, Beaulieu L, Carrier J, Castrovillari F, Chauvie S, Foppiano F, et al. Overview of Geant4 applications in medical physics. IEEE Nuc Sci Symp Conf Rec 2003:1743–5.
[8] Carrier JF, Archambault L, Beaulieu L, Roy R. Validation of GEANT4, an object-oriented Monte Carlo toolkit, for simulations in medical physics. Med Phys 2004;31:484–92.
[9] Amako K, Guatelli S, Ivanchenko VN, Maire M, Mascialino B, Murakami K, et al. Comparison of Geant4 electromagnetic physics models against the NIST reference data. IEEE Trans Nuc Sci 2005;52:910–8.
[10] Amako K, Guatelli S, Ivanchencko V, Maire M, Mascialino B, Murakami K, et al. Geant4 and its validation. Nuc Phys B – Proc. 2006;150:44–9.
[11] Constantin M, Constantin DE, Keall PJ, Narula A, Svatos M, Perl J. Linking computer-aided design (CAD) to Geant4-based Monte Carlo simulations for precise implementation of complex treatment head geometries. Phys Med Biol 2010;55(8):N211.
[12] El Bakkali J, El Bardouni T. Validation of Monte Carlo Geant4 code for a 6MV Varian linac. J King Saud Uni – Sci 2017;29:106–13.
[13] Sardari D, Maleki R, Samavat H, Esmaeeli A. Measurement of depth-dose of linear accelerator and simulation by use of Geant4 computer code. Rep Prac Onc Rad 2010;15:64–8.
[14] Heath E, Seuntjens J. Development and validation of a BEAMnrc component module for accurate Monte Carlo modelling of the Varian dynamic Millennium multileaf collimator. Phys Med Biol 2003;48:4045.
[15] Jang SY, Vassiliev ON, Liu HH, Mohan R, Siebers JV. Development and commissioning of a multileaf collimator model in Monte Carlo dose calculations for intensity-modulated radiation therapy. Med Phys 2006;33:770–81.
[16] Onizuka R, Araki F, Ohno T. Monte Carlo dose verification of VMAT treatment plans using Elekta Agility 160-leaf MLC. Phys Med 2018;51:22–31.
[17] Heidorn S-C, Kilby W, Fürweger C. Novel Monte Carlo dose calculation algorithm for robotic radiosurgery with multi leaf collimator: dosimetric evaluation. Phys Med 2018;55:25–32.
[18] Okamoto H, Fujita Y, Sakama K, Saitoh H, Kanai T, Itami J, et al. Commissioning of 6 MV medical linac for dynamic MLC-based IMRT on Monte Carlo code GEANT4. Radiol Phys Tech 2014;7:246–53.
[19] Arnfield MR, Siebers JV, Kim JO, Wu Q, Keall PJ, Mohan R. A method for determining multileaf collimator transmission and scatter for dynamic intensity modulated radiotherapy. Med Phys 2000;27:2231–41.
[20] Perales Á, Cortés-Giraldo MA, Miras H, Arráns R, Gallardo MI. Dosimetric impact assessment using a general algorithm in geant4 simulations for a complex-shaped multileaf collimator. Phys Med 2017;41:39–45.
[21] Borges C, Zarza-Moreno M, Heath E, Teixeira N, Vaz P. Monte Carlo modeling and simulations of the High Definition (HD120) micro MLC and validation against measurements for a 6 MV beam. Med Phys 2011;39:415–23.
[22] Borca VC, Pasquino M, Russo G, Grosso P, Cante D, Sciacero P, et al. Dosimetric characterization and use of GAFCHROMIC EBT3 film for IMRT dose verification. J Appl Clin Med Phys 2013;14(2):158–71.
[23] Villarreal- Barajas JE, Khan R. Energy response of EBT3 radiochromic films: implications for dosimetry in kilovoltage range. J Appl Clin Med Phys 2014;15(1):331–8.
[24] Ma CM, Li JS, Pawlicki T, Jiang SB, Deng J, Lee MC, et al. A Monte Carlo dose calculation tool for radiotherapy treatment planning. Phys Med Biol 2002;47(10):1671–89.
[25] Siebers JV, Keall PJ, Kim JO, Mohan R. A method for photon beam Monte Carlo multileaf collimator particle transport. Phys Med Biol 2002;47(17):3225–49.